

## EFFECT OF FIBER TYPES ON SHEAR PERFORMANCE OF PRECAST CONCRETE BEAM-COLUMN JOINTS USING DFRCC

H. Yamada<sup>1</sup>, M. Ando<sup>1</sup>, A. Yasojima<sup>2</sup>, and T. Kanakubo<sup>3</sup>

<sup>1</sup> Master Program, Dept. of Engineering Mechanics and Energy, University of Tsukuba, Japan

<sup>2</sup> Associate Professor, Dept. of Engineering Mechanics and Energy, University of Tsukuba, Japan

<sup>3</sup> Professor, Dept. of Engineering Mechanics and Energy, University of Tsukuba, Japan

**ABSTRACT:** In this study, the loading test of PCa beam-column joints using DFRCC in panel zone was conducted to evaluate the effect of shear performance of joint panel. The main parameters are the fiber type (PVA and steel) and fiber volume fraction (1.0% and 2.0%) in mortar matrix. From the experiment results, it can be recognized that the maximum load of beam-column joint increased by mixing fiber, and the fiber bridging effect of PVA fiber and steel fiber were different. According to the image analysis of observed cracks in panel zone, shear force that is carried by fibers can be calculated from the bridging law of PVA fiber and results of uniaxial tension test of DFRCC with steel fiber. In the case of PVA fiber, the calculated shear force showed a good agreement with the test results. On the other hand, the calculated shear force disagreed with the experimental results in the case of steel fiber.

### 1 INTRODUCTION

Construction method using precast (PCa) members has been more common for the skyscraper buildings to rationalize workmanship. Up to now, new PCa system, in which the panel zone of the beam-column joint is also manufactured as a PCa member in factory, has been proposed. On the other hand, many researches on ductile fiber-reinforced cementitious composites (DFRCC), which has a high ductility, have been carried out in recent years (Japan concrete institute, 2012). Previous study reported that DFRCC used in panel zone can inhibit the damage of joint panel and increase the maximum load (Sano et al., 2015). It is also considered that the shear force carried by fiber can be calculated by evaluating the behavior of cracks in panel zone and using bridging law.

In this study, the loading test of PCa beam-column joints using DFRCC in panel zone, which are designed to fail by shear failure in panel zone before flexural yielding, was conducted to evaluate the effect of fiber types on shear performance and crack behavior of joint panel.

## 2 EXPERIMENTAL PROGRAM

### 2.1 Test specimens

Table 1 shows the specimens list. The dimension of the specimens is shown in Figure 1. Specimens No.26, 27, 28 and 29 are tested in this study and specimens No.24 and No.25, of which results have been reported in the previous study (Sano et al., 2015), are also included to discuss. The internal beam-column joint in skyscraper RC buildings is scaled with the beam section of set up 380 mm × 420 mm and the column section of 500 mm × 500 mm. The specimens are designed to fail by shear in joint panel before flexural yielding in order to evaluate the shear capacity of panel zone. Therefore, the safety margin of shear capacity of joint panel is set at approximately 0.6 by using high strength bars in beam and column. The main parameters are the fiber type (PVA and steel) and fiber volume fraction (1.0% and 2.0%) in mortal matrix of panel zone. For specimens No.26 and No.27, PVA fiber with 1% and 2% of volume fraction was used. Specimens No.28 and No.29 were manufactured using steel fiber with 1% and 2%. Specimen No.26 was designed as the specimen with hoops in panel zone area. Mechanical properties of PVA fiber and steel fiber are shown in Table 2. The results of material tests for concrete, DFRCC and reinforcing bars are summarized in Table 3 and Table 4.

**Table 1. Specimen list**

ID	Panel Zone				Beam		Column	
	Target strength (MPa)	Fiber type	Fiber volume fraction (%)	Hoop	Longitudinal reinforcing bar	Stirrup	Longitudinal reinforcing bar	Hoop
No.24 No.25	40	-	0.0	-				
No.26 No.27		PVA fiber	1.0 2.0	6-D10@60 (SD785)	18-D22 (USD685)	6-D10@60 (SD785)	16-D22 (USD685)	6-D10@60 (SD785)
No.28 No.29		Steel fiber	1.0 2.0	-				

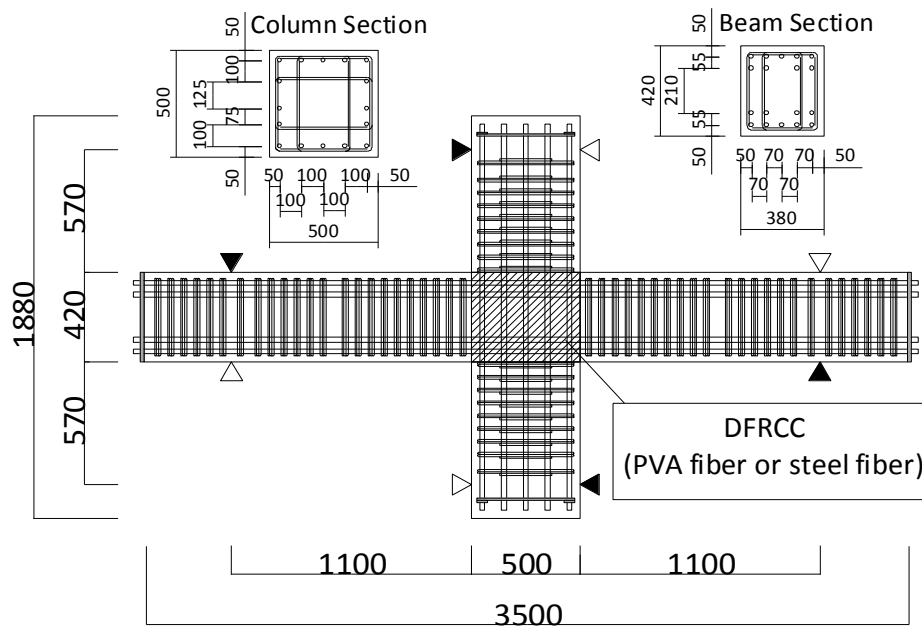


**Figure 1. Specimen dimensions.**

**Table 2. Mechanical properties of fiber**

Fiber	Length (mm)	Diameter (mm)	Tensile strength (MPa)	Elastic modulus (GPa)
PVA	12	0.10	1200	28
Steel	13	0.16	2830	210

**Table 3. Mechanical properties of concrete and DFRCC**

Type	Specimen No	Place	Compressive strength (MPa)	Splitting tensile strength (MPa)	Elastic modulus (GPa)
Concrete	No.26	Beam and	54.6	3.71	29.5
	No.27	Column	57.1	3.03	30.5
DFRCC (PVA fiber)	No.26	Panel zone	52.9	-	15.6
	No.27		50.0	-	15.7
Concrete	No.28	Beam and	89.4	5.57	38.4
	No.29	Column	88.6	4.42	39.0
DFRCC (steel fiber)	No.28	Panel zone	56.8	-	18.7
	No.29		59.2	-	19.6

**Table 4. Mechanical reinforcing of bar**

Specimen No	Type	Diameter	Note	Yield strength (MPa)	Tensile strength (MPa)	Elastic modulus (GPa)
No.26	USD685	D22 (22 mm)	Longitudinal reinforcing bar	717	899	192

No.27	SD785	D10 (10 mm)	Stirrup and hoop in Column and Beam	833	991	216
No.26	SD295	D10 (10 mm)	Hoop in Panel Zone	346	468	192
No.28	USD685	D22 (22 mm)	Longitudinal reinforcing bar	712	898	189
No.29	SD785	D10 (10 mm)	Stirrup and hoop in Column and Beam	833	1047	209

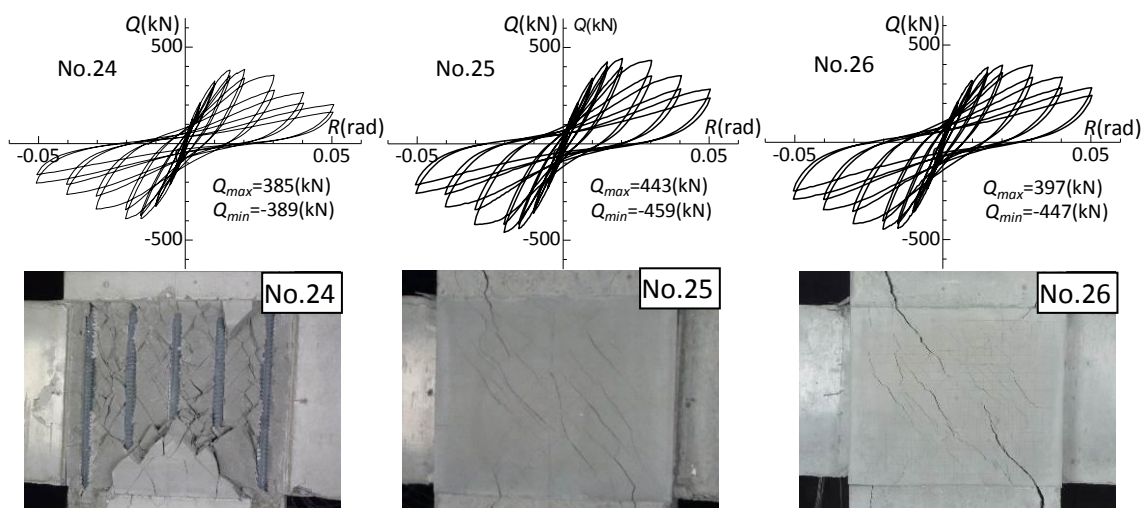
## 2.2 Loading method and measurement

The inflection points of the columns were supported by oil jacks and the story drift angle was controlled by the actuators attached to the inflection points of the beams. The reversed cyclic loading was applied with the target story drift angles of  $R=\pm 1/400, \pm 1/200, \pm 1/100, \pm 1/67, \pm 1/50, \pm 1/33, \pm 1/25$  and  $\pm 1/20$ . In this study, to observe shear cracks behavior in panel zone, photos were taken using two cameras during the loading (details are explained in Chapter 4).

## 3 EXPERIMENTAL RESULT

### 3.1 Load-story drift angle curve and failure mode

Figure 2 shows the relationship between the applied load to beam and the story drift angle, and shows the failure mode of the panel zone at the maximum load. Shear cracks in panel zone and those in beams occurred in all specimens. After that, the shear crack width in panel zone increased. The maximum load of No.26 and No.27 was observed at  $1/50$  rad, and that of No.28 and No.29 was observed at  $1/33$  rad. After the maximum load, although the shear cracks opened in panel zone of all specimens, damage of joint panel was inhibited comparing with specimen No.24, which is without fiber in panel zone. It can be recognized that the maximum load of beam-column joint increased by mixing fiber. The maximum load of specimens with steel fiber are higher than that of specimens with PVA fiber. It can be also recognized that the fiber bridging effect of PVA fiber differs from that of steel fiber. From the comparison between specimens No.25 and No.26, of which maximum load is 459kN and 447kN respectively, hoops arrangements do not affect the maximum load. This leads that hoops in panel zone do not affect significantly shear capacity of joint panel using DFRCC.



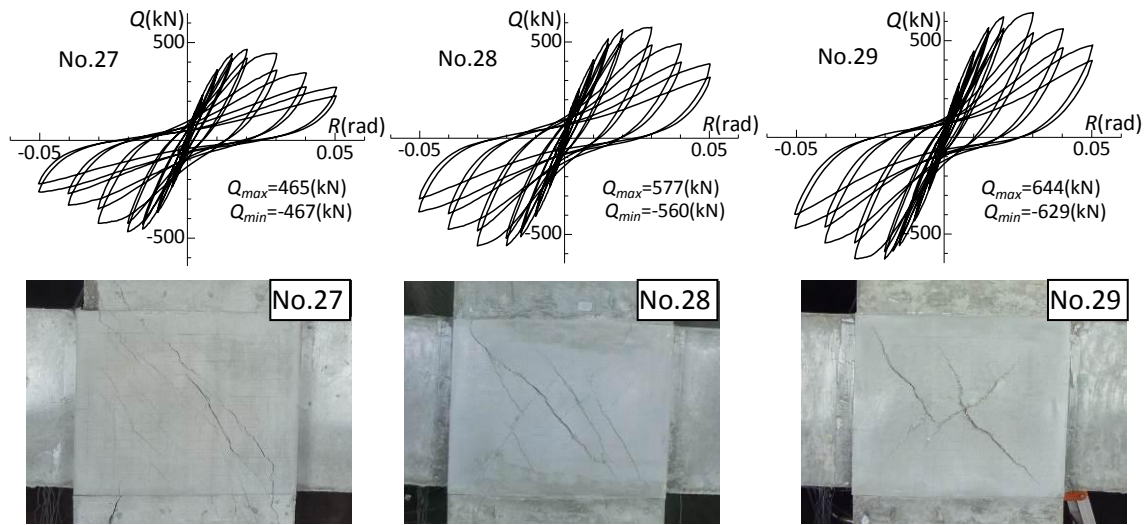


**Figure 2. Load – story drift angle curve and crack pattern ( $R=1/33\text{rad.}$ ).**

#### 4 CRACK BEHAVIOR IN PANEL ZONE

##### 4.1 Method of observation

To evaluate the crack behavior in panel zone, photos of panel zone with the mesh of 10 mm x 10 mm intervals on the surface were taken by two cameras as shown in Figure 3. The target photographing regions were top left and bottom right area (120 mm x 80 mm). 1 pixel corresponds to 0.02 mm square.

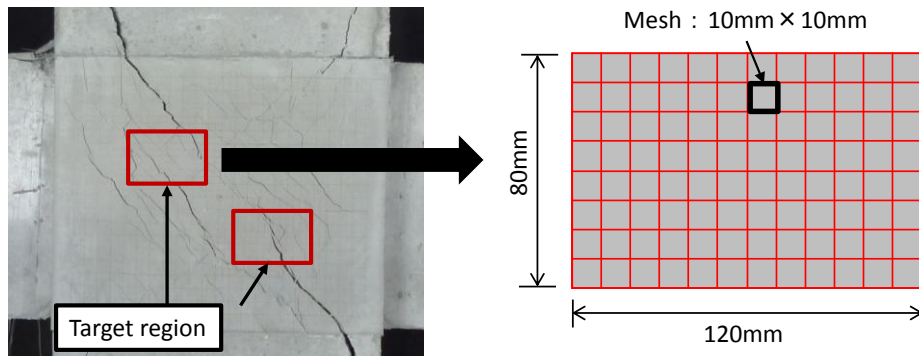


**Figure 3. Target region.**

##### 4.2 Crack behavior

The calculation method of crack width is shown in Figure 4. It is considered that the panel zone has a biaxial stress field in which tensile stress and shear stress are distributed along shear crack. The crack width is defined as the relative displacement between two points printed in same mesh line. Crack opening and crack sliding is severally defined as the normal movement and the parallel displacement with crack plane between two points.

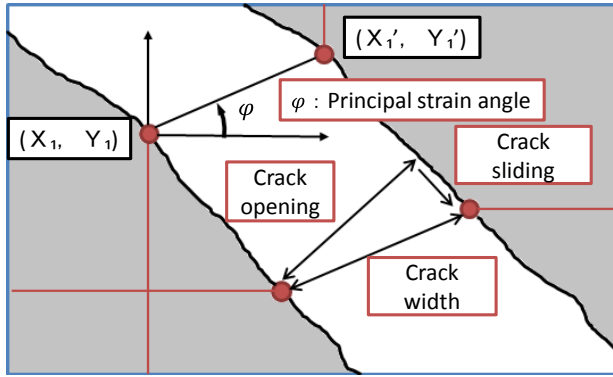


Figure 4. Calculation method of crack.

Observed cracks of each specimen are indicated in Figure 5. Figure 6 shows the development of crack width, crack opening, crack sliding and principal strain angle. The plotted marks are the peak values of each first loading cycle. The crack width spread with an increase in the story drift angle. The crack width of specimen No.26 and No.27 with PVA fiber attains approximately 0.8mm at maximum load that the story drift angle reaches 1/50 rad. After the maximum load, the crack width increase furthermore and reaches around 4-6mm at most. On the other hand, although the crack width of specimen No.28 and No.29 with steel fiber is small until 1/50 rad. of story drift angle, the width increases remarkably at maximum load in 1/33 rad. At the maximum load, the crack width reaches approximately 2-4mm which is considerable larger than that of No.26 and No.27 and the width increases furthermore after that. Both the crack opening and the crack sliding of all specimens increase as the target story drift angle also increases. However, the values of crack sliding are smaller than crack opening until the maximum load.

The principal strain angle is around 40 degrees when cracks appear on the surface of panel. Although the angle increases as the story drift increases, the angle decreases after maximum load. The difference of principal strain angle between No.28 and No.29 was not clearly confirmed. From those results, it is considered that fiber volume fraction does not affect the principal strain angle. The principal strain angle of No.26 which has hoops in panel zone is smaller than that of No.27 without hoops. It is considered that is due to horizontal restraint effect of hoops.

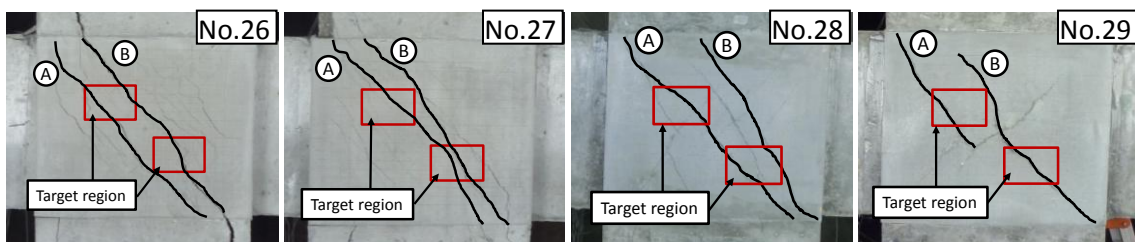
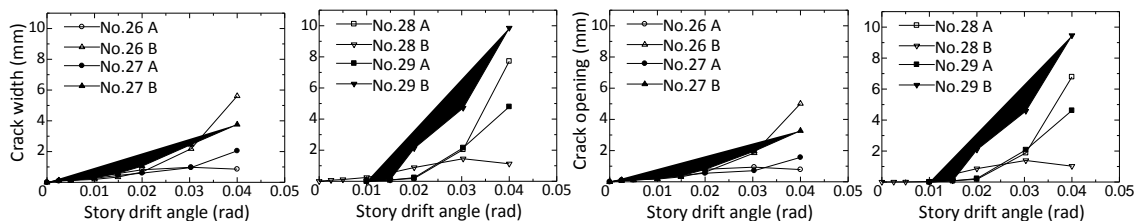
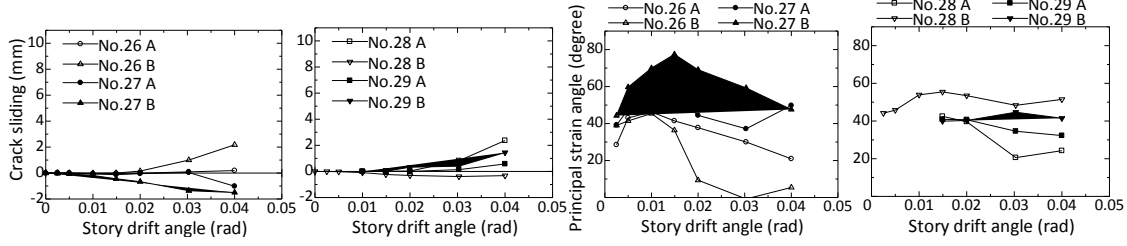


Figure 5. Observed cracks





**Figure 6. Crack behavior**

## 5 SHEAR FORCE CARRIED BY FIBER

### 5.1 Calculation method

The calculation process of shear force carried by fiber is shown in Figure 7. The shear force carried by fiber is derived from the crack width and the principal strain angle explained before. The tensile stress and tensile force are calculated using these values, which are defined as the averages of those of neighbor two points for target crack. The sectional area generating these stresses is assumed as the area between the two points. The tensile stress carried by fibers across cracks can be calculated from the bridging law of PVA fiber (Asano et al., 2014) and the results of uniaxial tension test of DFRCC with steel fiber (the upper right figure in Figure 7). Uniaxial tension test was carried out using the specimen with the same shape as previous report (Tsukizaki et al., 2014.). The bridging law of PVA fiber is calculated using same method with the previous study (Kanakubo et al. 2016) based on the assumption that fiber orientation distribution is given as same with uniaxial tension test.

The tensile force is estimated from tensile stress multiplied by the sectional area. The sectional area generating tensile stress is assumed to be crack surface between mesh lines with the principal strain angle. The fiber shear force is obtained as the horizontal component of tensile force. Panel shear force carried by fiber is summed for all of the forces in each mesh. It is assumed that the cracks out of the photo areas show the same behavior with those in the photo area.

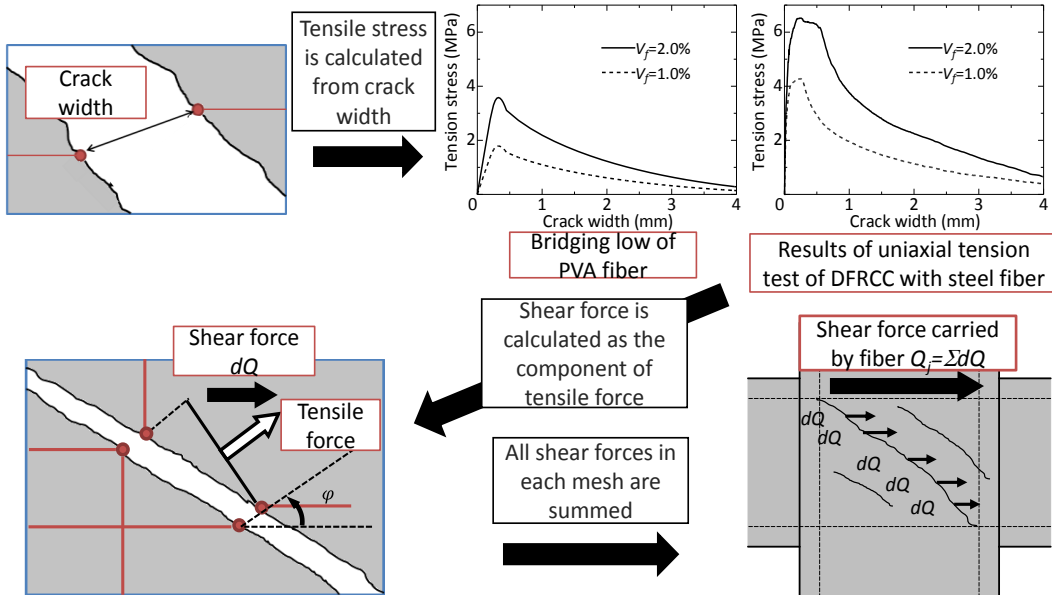


**Figure 7. Derivation process of shear force by fiber**

### 5.2 Comparison of shear force carried by fiber

Figure 8 shows the transitions of the shear force differences between specimens No.25 and No.27 for PVA fiber, and specimens No.28 and No.29 for steel fiber. The straight lines show the difference in

calculated shear force given by the method explained before, and the dotted lines show the shear force difference from the test results. Calculation results are defined as the average shear force from two cracks shown in Figure 5. The calculated ones between specimens No.28 and No.29 from  $1/67$  rad. to  $1/33$  rad. of story drift angle are only shown in the figure, because cracks could not be observed up to  $1/67$  rad. and the calculated tensile stress is zero over  $1/33$  rad. due to rapid expansion of crack width in No.29.

Comparison of specimens No.25 and No.27 with PVA fiber shows that the calculated shear force had a good agreement with the test results. On the other hand, in comparison of specimens No.28 and No.29, although the calculated shear force show a good agreement with the test results until story drift angle of  $1/50$  rad., the calculated value disagreed with the experimental results after that angle. It is considered that steel fiber has larger effect of fiber bridging across cracks than PVA fiber due to no rupture behavior of steel fiber. It is assumed that shear resistance caused by crack sliding does not give considerable effect because crack sliding is small until story drift of  $1/50$  rad. After increasing of crack sliding, shear resistance caused by crack sliding assumed to increase. Therefore, it is considered that calculated shear force underestimates test results after  $1/50$  rad. of story drift angle.

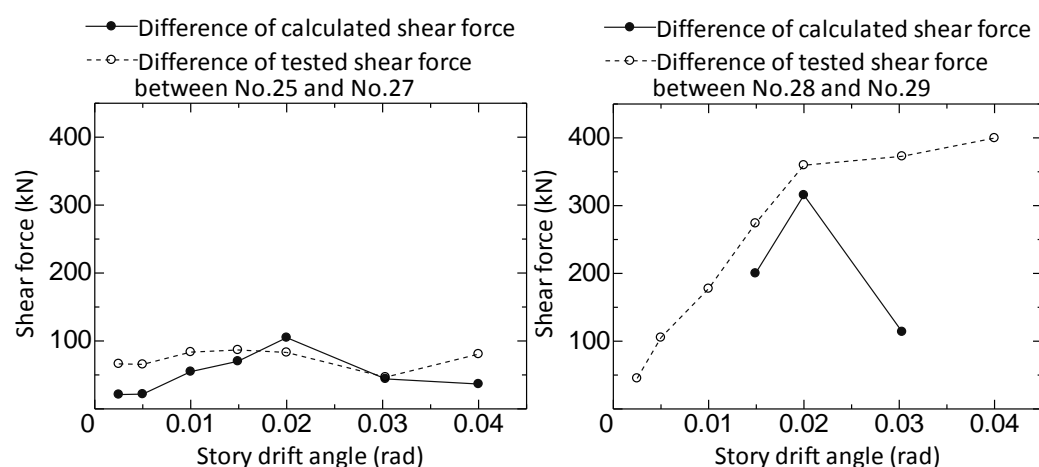


**Figure 8. Comparison of shear force carried by fibers**

## 6 CONCLUSION

In this study, the loading test of specimens using DFRCC in panel zone was conducted to evaluate the effect of fiber types on shear performance. The maximum load of specimens with steel fiber are higher than specimens with PVA fiber. According to the image analysis of observed cracks in panel zone, shear force carried by fibers is calculated from the bridging law of PVA fiber and results of uniaxial tension test of DFRCC with steel fiber. In the case of PVA fiber, the calculated shear force showed a good agreement with the test results. On the other hand, the calculated shear force disagreed with the experimental results in the case of steel fiber. It is considered that the fiber bridging effect of PVA fiber differs from that of steel fiber.

## 7 ACKNOWLEDGEMENT

The authors wish to express their gratitude and sincere appreciation to the Tokyoutekkou Co., Ltd. for providing the experiment materials. This study was supported by the JSPS KAKENHI Grant Number 26289188.



## 8 REFERENCES

- Asano, K. and Kanakubo, T. (2014) "Study on Fiber Bridging Constitutive Law in Consideration of Fiber Orientation in High Performance Fiber Reinforced Cementitious Composites", *Summaries of technical papers of annual meeting Architectural Institute of Japan, Materials and Construction*, pp. 185-186. (in Japanese)
- Japan Concrete Institute (2012) "Technical Committee Report on Innovation Application of Fiber Reinforced Cementitious Composites", *Committee Report JCI-TC-104A*, (in Japanese)
- Kanakubo, T., Miyaguchi, M. and Asano, K. (2016) "Influence of Fiber Orientation on Bridging Performance of Polyvinyl Alcohol Fiber - Reinforced Cementitious Composite", *ACI Materials Journal*, Vol.133, No.2, pp.131-141.
- Sano, N., Yamada H., Miyaguchi, M., Yasojima, A. and Kanakubo, T. (2015) "Structural Performance of Beam-Column Joint using DFRCC" *The 11<sup>th</sup> Canadian Conference on Earthquake Engineering-Facing Seismic Risk*-, PaperID:94163
- Tsukizaki, R., Miyaguchi, M., Wan, Z., Asano, K. and Kanakubo, T. (2014) "Study on Fiber Orientation of HPRCC: Part1: Experimental results of tension and bending tests", *Summaries of technical papers of annual meeting Architectural Institute of Japan, Materials and Construction*, pp. 179-184. (in Japanese)